Article

Cell Reports

Shaping of Intestinal Microbiota in Nlrp6- and Rag2-Deficient Mice Depends on Community Structure

Graphical Abstract

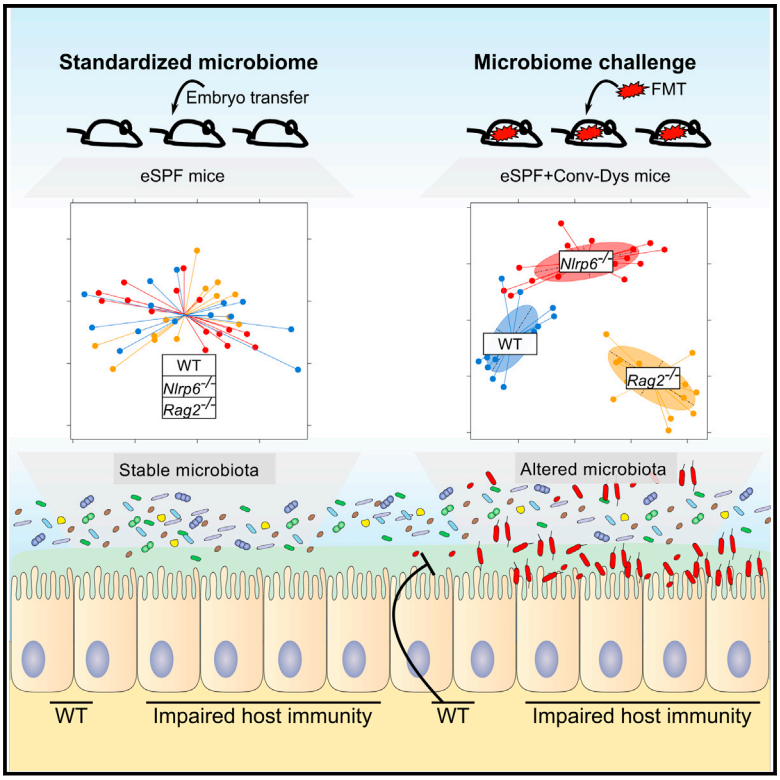

Authors

Eric J.C. Gálvez, Aida Iljazovic, Achim Gronow, Richard Flavell, Till Strowig

Correspondence

till.strowig@helmholtz-hzi.de

In Brief

Through analysis of intestinal microbiota composition after normalization and after experimental alteration, Galvez et al. demonstrate that, in mice, the impact of distinct immune components such as Nlrp6 and adaptive immunity strictly depends on the community structure of the ecosystem.

Highlights

- Familial transmission influences microbiota composition in Nlrp6-deficient mice
- In pathobiont-free conditions, WT, *Nlrp6*$^{-/-}$, and *Rag2*$^{-/-}$ mice have a similar microbiota
- Effect of host immunity on microbiota is detectable upon introduction of pathobionts
- Genotype, environmental, and ecological factors together shape microbial colonization

Gálvez et al., 2017, Cell Reports *21*, 3914–3926
December 26, 2017
https://doi.org/10.1016/j.celrep.2017.12.027

CellPress

OPEN ACCESS
CellPress

Cell Reports
Article

Shaping of Intestinal Microbiota in Nlrp6- and Rag2-Deficient Mice Depends on Community Structure

Eric J.C. Gálvez,[1] Aida Iljazovic,[1] Achim Gronow,[1] Richard Flavell,[2,3] and Till Strowig[1,4,*]
[1]Research Group Microbial Immune Regulation, Helmholtz Centre for Infection Research, Braunschweig, Germany
[2]Department of Immunobiology, Yale University School of Medicine, New Haven, CT 06520, USA
[3]Howard Hughes Medical Institute, Yale University, New Haven, CT 06520, USA
[4]Lead Contact
*Correspondence: till.strowig@helmholtz-hzi.de
https://doi.org/10.1016/j.celrep.2017.12.027

SUMMARY

Contradicting observations have been made regarding the relative contributions of immune sensors to shaping the microbiome, yet the reasons for these discrepancies are not fully understood. Here, we investigated the contribution of environmental factors in shaping the microbiome in mice deficient in adaptive immunity (*Rag2*$^{-/-}$) and Nlrp6, an immune sensor proposed to be involved in regulation of microbiota composition. In conventionally housed *Nlrp6*$^{-/-}$ mice, familial transmission has a significant effect on microbiota composition, complicating the analysis of genotype-dependent effects. Notably, after rederivation into standardized specific pathogen-free (SPF) conditions devoid of pathobionts, microbiota composition was indistinguishable between WT, *Rag2*$^{-/-}$, and *Nlrp6*$^{-/-}$ mice. However, upon reintroduction of a pathobiont-containing community host, genotype-dependent differences reappear, specifically affecting the relative abundance of pathobionts such as *Helicobacter spp*. Our results show that the impact of Nlrp6 and also of adaptive immunity on microbiota composition depends on community structure and primarily influences pathobionts but not commensals.

INTRODUCTION

The microbiota encompasses diverse populations of bacteria, archaea, and eukaryota that populate many body sites of multicellular hosts, with the gastrointestinal (GI) tract harboring a large majority of microbes in humans (Simon and Gorbach, 1984). Each of these microbial ecosystems is dynamically shaped by numerous factors, and, consequently, differences at all phylogenetic levels have been reported between individuals and populations around the globe (Clemente et al., 2015). Many of these differences derive from the diverse environmental conditions in which humans live, resulting in exposure to different microbes, but contributions of genetic factors have also been identified for a limited set of genes and microbes (Goodrich et al., 2014). Hence, in emerging models, the composition of the microbiota of each individual is considered a complex phenotype influenced by both environmental and host factors, which are, in many cases, interconnected, making it difficult to distinguish associations from causal relationships.

We have previously shown that deficiency in the Nlrp6 inflammasome results in distinct alterations of the microbiota that are disease exacerbating in mouse models of inflammatory bowel disease (IBD), intestinal tumorigenesis, and metabolic dysfunction (Elinav et al., 2011; Henao-Mejia et al., 2012; Hu et al., 2013). Similar observations were made for other immune sensors such as TLR5 and NOD2, as well as adaptive immunity (Rehman et al., 2011; Vijay-Kumar et al., 2010; Zhang et al., 2015). However, conflicting results have been reported, raising doubts as to whether distinct host-immune deficiencies directly cause aberrations in the gut microbiota or whether they rather reflect the influence of environmental factors such as familial transmission (Mamantopoulos et al., 2017; Robertson et al., 2013; Ubeda et al., 2012). Alternatively, it can be hypothesized that contradictory results are caused by differences in the experimental setup, including the composition and structure of the respective evaluated microbial ecosystems. Consequently, distinct alterations may not be detectable under all conditions tested. Along these lines, a recent study has challenged the proposed role of the Nlrp6 inflammasome in shaping the microbiome, claiming that a generalizable impact of this Nlrp6 was not detectable upon rederivation of these mice into specific pathogen-free (SPF) conditions (Mamantopoulos et al., 2017). Whether the Nlrp6 inflammasome and other parts of the immune systems, such adaptive immunity, are general regulators of microbiome structure or, rather, influence the structure of the community only under specific conditions is currently not known.

Hence, we investigate here the contribution of Nlrp6 and adaptive immunity on the composition of the intestinal microbiome, using three distinct approaches. First, a large-scale cross-sectional study of conventionally housed *Nlrp6*$^{-/-}$ mice was performed to estimate the influence of genotype, familial transmission, and cage effects. Second is the rederivation of gene-deficient *Nlrp6*$^{-/-}$ and *Rag2*$^{-/-}$ mice into standardized enhanced specific pathogen-free (eSPF) conditions devoid of

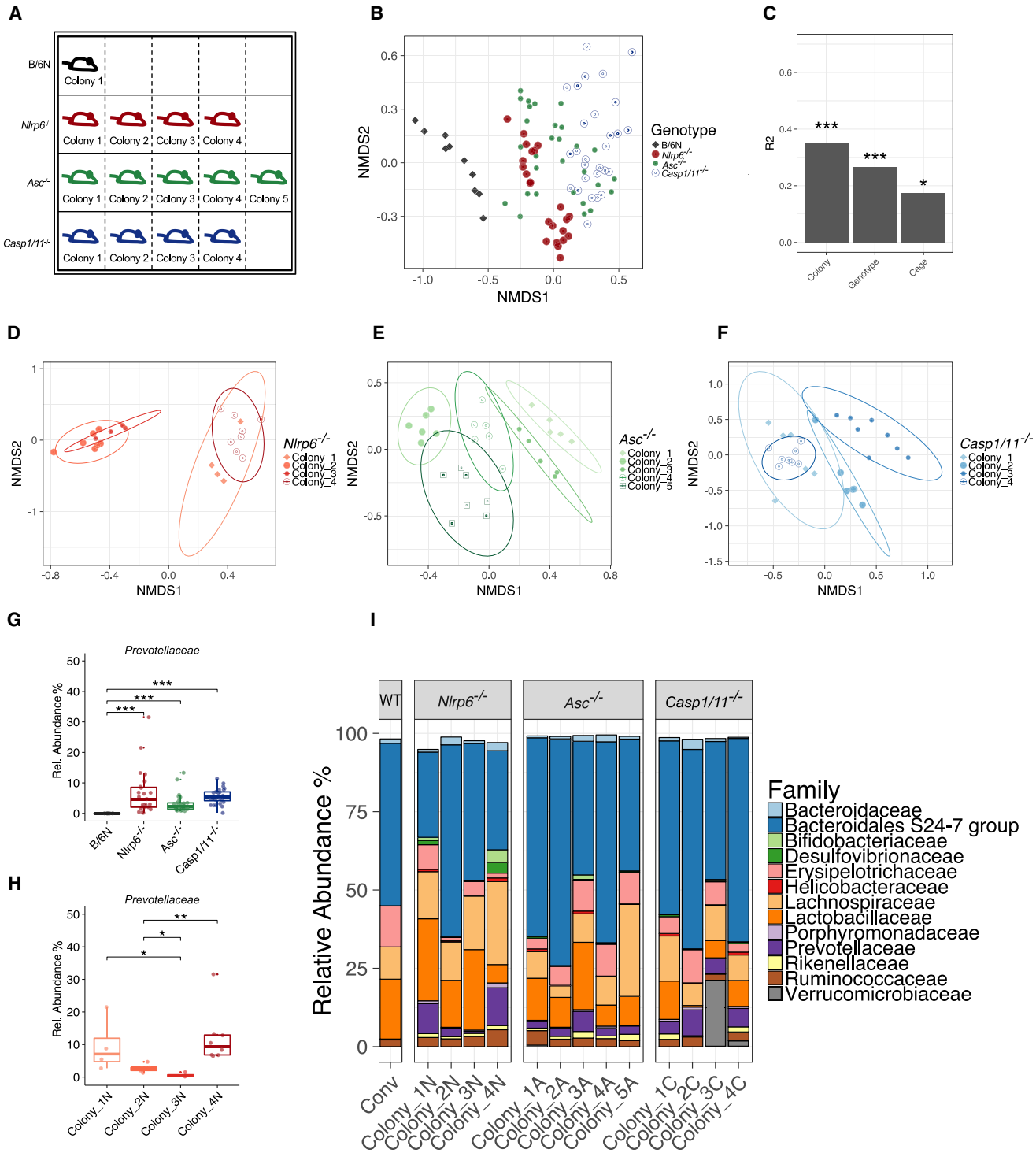

Figure 1. Environmental Factors Contribute to Diverse Microbiota Composition in Nlrp6 Inflammasome-Deficient Mice

(A) Scheme for cross-sectional characterization of fecal microbiota composition in WT, *Nlrp6*$^{-/-}$, *Asc*$^{-/-}$, and *Casp1/11*$^{-/-}$ mice maintained by inbreeding in conventional housing conditions.

(B) NMDS ordination analysis of microbiota composition in mice using Bray-Curtis distances grouped by genotype.

(C) Individual effect size of tested covariates.

(D–F) NMDS ordination analysis of microbiota composition in *Nlrp6*$^{-/-}$ (D), *Asc*$^{-/-}$ (E), and *Casp1/11*$^{-/-}$ (F) mice using Bray-Curtis distances grouped by colony. Ellipses indicate dispersion of samples within colony.

(legend continued on next page)

known pathobionts. Finally, we analyzed the dynamic assembly of the microbiota upon controlled introduction of a dysbiotic community into isobiotic wild-type (WT) and gene-deficient mice, using 16S rRNA gene sequencing to specifically survey the structure and composition of metabolically active bacteria. Our results highlight the large effect of familial transmission on community structure that has not previously been demonstrated for Nlrp6 inflammasome-deficient mice affecting the presence of numerous bacterial families, including Prevotellaceae and Helicobacteraceae. Moreover, characterization of mice raised in eSPF conditions revealed that neither Nlrp6 nor adaptive immune cells contribute to shaping the microbiota composition under these conditions. However, upon reintroduction of a dysbiotic community into isobiotic WT, *Nlrp6*$^{-/-}$, and *Rag2*$^{-/-}$ mice, distinct differences in the composition of the metabolically active microbiota became detectable, suggesting that Nlrp6 and adaptive immunity specifically contribute to the regulation of microbiota composition in the presence of microbes with proinflammatory features.

RESULTS

Familial Transmission Significantly Influences Microbiota Composition in Conventionally Housed Nlrp6 Inflammasome-Deficient Mice

Using a cross-sectional study of distinct lines of WT and gene-deficient mice, we previously identified an altered microbial community in Nlrp6 inflammasome-deficient mice (Elinav et al., 2011). Taking into account recent advances in the understanding of the contribution of environmental and experimental variables on microbiome composition (Rausch et al., 2016; Stappenbeck and Virgin, 2016; Ubeda et al., 2012), we wanted to estimate the influence of host genetics and familial transmission in mice deficient in components of the Nlrp6 inflammasome. To this end, we surveyed microbiome composition in mice from 13 colonies of Nlrp6-, Asc-, and caspase-1-deficient mouse lines as well as one colony of WT mice (n = 4–10 mice per group) (Figure 1A). All the colonies were housed in several different rooms within one large animal facility using conventional housing conditions (Experimental Procedures). The fecal microbiota was characterized by 16S rRNA gene sequencing, followed by ordination analyses using Bray-Curtis dissimilarity distances. Non-metric multidimensional scaling (NMDS) revealed a complex pattern of community structures (Figure 1B). We used permutational multivariate ANOVA (ADONIS), considering the factors "genotype," "colony," and "cage" to evaluate their relative contribution to variability within the microbiota. This analysis identified that gene-deficient mice clustered distinctively, compared to WT mice bred and maintained in the same facility (Figure 1C; $R^2 = 0.265$, $p < 0.001$). However, an even larger effect was noted to derive from the factor "colony" ($R^2 = 0.349$, $p < 0.001$). Notably, the factor "cage" had a lower but significant effect, compared to "genotype" ($R^2 = 0.172$, $p < 0.05$). Finally, when only comparing mice with the same genotype, we confirmed that association with different colonies explained a large fraction of the variability in microbiota composition in *Nlrp6*$^{-/-}$, *Asc*$^{-/-}$, and *Casp1/11*$^{-/-}$ mice (Figures 1D–1F; R^2s = 0.487, 0.555, and 0.408, respectively; $p < 0.001$). Prevotellaceae, which we previously identified to be enriched in *Nlrp6*$^{-/-}$ mice (Elinav et al., 2011), had the highest abundance in *Nlrp6*$^{-/-}$ mice compared to WT, *Asc*$^{-/-}$, and *Casp1/11*$^{-/-}$ mice (Figure 1G), but significant differences were observed in colonies of *Nlrp6*$^{-/-}$ mice (Figure 1H; $p < 0.001$, Kruskal-Wallis test). Moreover, operational taxonomic units (OTUs) belonging to the genus Prevotella differed strongly between mouse lines and even colonies further supporting the high variability in the microbiome of these lines (Figure S1). Beside the genus *Prevotella*, similar colony-specific alterations in the abundance of distinct bacterial families were observed in many colonies of gene-deficient mice (Figure 1I), e.g., high abundances of Verrucomicrobiaceae and Helicobacteraceae in individual colonies but that were largely absent in other colonies (Figure S1). Importantly, this cross-sectional study of mice bred under conventional housing conditions highlighted that segregation of mouse lines even within the same facility and kept under the same hygiene conditions has a tremendous impact of microbiota composition, such as the presence or absence of putative pathobionts, including *Prevotella spp*., *Helicobacter spp*., and *Akkermansia muciniphilia*. This supports the model that, beyond genotype, additional factors such as maternal inheritance and stochastic events influence the composition of the microbiome in conventionally housed mice, even when they are maintained within the same facility.

Rederivation into Enhanced SPF Conditions Diminishes the Effect of Nlrp6 Deficiency on Microbiota Composition

Standardization of microbiota composition has recently been proposed as an approach to overcome microbiota variability in animal experimentation (Macpherson and McCoy, 2015). In order to assess the microbiota composition in WT and gene-deficient mice under controlled environmental conditions, we used rederivation of mice by embryo transfer (ET) through a cohort of foster mothers with a semi-standardized microbiota (Figure 2A; Experimental Procedures). We focused our initial analysis on two strains of gene-deficient mice, the aforementioned *Nlrp6*$^{-/-}$ mice as well as mice deficient in Rag2 (*Rag2*$^{-/-}$), thereby lacking adaptive immunity. The latter strain was included, since previous studies had reported conflicting results on the type of alterations in microbiota composition in these mice (Garrett et al., 2007; Zhang et al., 2015). Specifically, we compared the composition of the fecal microbiota in two cohorts of WT, *Rag*$^{-/-}$, and *Nlrp6*$^{-/-}$ mice each, one cohort before and one cohort after ET. NMDS analysis showed two main clusters corresponding to the samples before (Figure 2B, Conv [conventionally housed) and after (Figure 2B, eSPF) ET. As observed before, mice maintained under conventional housing (Figure 2B, Conv) clustered by genotype. In

(G and H) Relative abundance of the family Prevotellaceae in mice grouped by genotype (G) and in *Nlrp6*$^{-/-}$ mice grouped by colony (H).
(I) Relative mean abundances of bacterial families in mice grouped by colony.
Permutational multivariate ANOVA (ADONIS) was used to calculate the variance explained by individual factors in (C). Mann-Whitney U test was used for (G) and (H). *p < 0.05; **p = 0.01; ***p < 0.001.

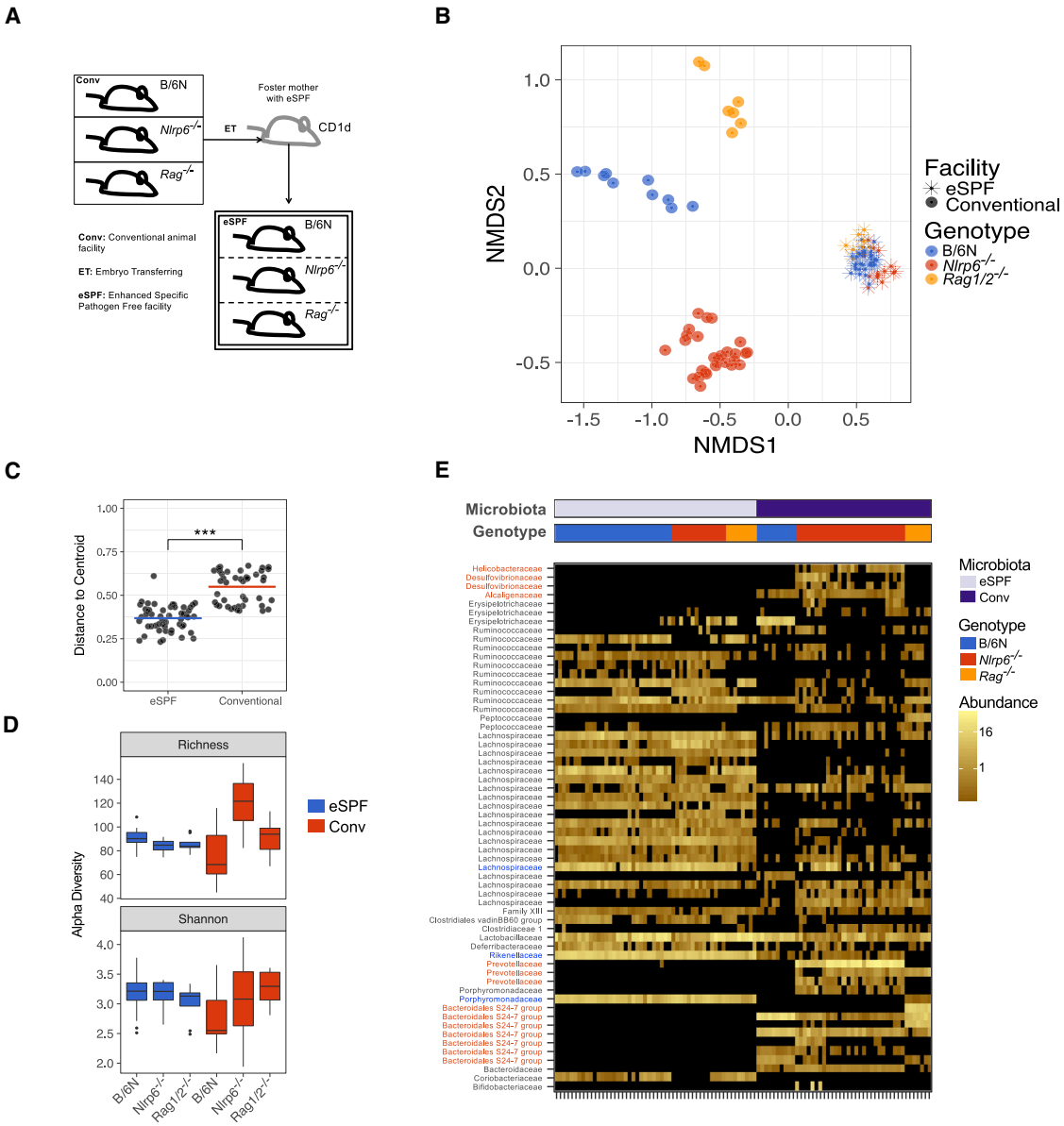

Figure 2. Rederivation of Immunodeficient Mice from Conventional Housing Conditions to eSPF Conditions Normalizes the Microbiota

(A) Scheme for rederivation of conventionally housed (Conv) mouse strains into enhanced SPF (eSPF) housing conditions via ET using CD1d foster mothers with eSPF microbiota.

(B–E) Fecal samples were obtained from Conv-housed (circles) and eSPF-housed (asterisks) mice of indicated genotypes.

(B) NMDS ordination analysis of microbiota composition using Bray-Curtis distances.

(C) Similarity analysis of microbiota composition within housing condition using Bray-Curtis distances to the respective centroid.

(D) Estimation of α-diversity using the richness and inverse Simpson indices. The dots indicate the outlayers.

(E) Heatmap of detected OTUs clustered at family level; the samples were grouped by housing condition (Microbiota) and genotype as indicated.

Mann-Whitney U test was used in (C). ***$p < 0.001$.

contrast, rederivation of *Rag2*$^{-/-}$ and *Nlrp6*$^{-/-}$ mice resulted in offspring with no obvious differences in gut microbiota composition as compared to WT mice (Figure 2B). Variability between samples were calculated using Bray-Curtis distances to the respective centroids (eSPF and Conv) demonstrating that beta diversity within eSPF mice is significantly lower than within Conv mice (Figure 2C; $p < 0.001$, Mann-Whitney test). Notably, mice with the eSPF microbiota have a similar alpha diversity compared to Conv mice (Figure 2D). However, while the eSPF microbiota contains mainly Firmicutes and only two families of Bacteroidales (Rikenellaceae and Porphyromonadaceae), Conv mice contain a larger fraction of distinct Bacteroidales families, e.g., Prevotellaceae and S24-7, as well as several representatives from the phylum Proteobacteria, including pathobionts from the families

Desulfovibrionaceae, Alcaligenaceae, and Helicobacteraceae (Figure 2E) (Palm et al., 2014; Sonnenberg et al., 2012). Next, we wanted to characterize whether other deficiencies in inflammasome components (*Nlrp3*$^{-/-}$, *Nlrp6*$^{-/-}$, *Asc*$^{-/-}$, *Casp1*$^{-/-}$, *Casp11*$^{-/-}$, *Casp1/11*$^{-/-}$, *Il1a*$^{-/-}$, and *Il1b*$^{-/-}$ mice) or specific subsets of adaptive immune cells (*Tcrb*$^{-/-}$*Tcrd*$^{-/-}$ and *muMT*$^{-/-}$ *Rag2*$^{-/-}$ mice) result in genotype-specific clustering when colonized with the eSPF microbiota. Analysis of microbiota composition in 336 mice from 13 colonies revealed that samples from individual mice were interspersed between genotypes without obvious clustering (Figures S2A and S2B). Specifically, genotype did not contribute significantly to the variation observed between WT mice and mice with inflammasome-related deficiencies ($R = 0.040$, $p = 0.106$, ANOSIM) as well as deficiencies in adaptive immune cell subsets ($R = 0.154$, $p = 0.002$, ANOSIM). The relative abundance of bacterial families remained comparable between all screened eSPF mice across 1 year of breeding (Figures S2C and S2D). This indicates that, under SPF conditions, Nlrp6-dependent effects on the microbiome are not detectable, which is in accordance with the recent study from Mamantopoulos and colleagues (Mamantopoulos et al., 2017). However, this observation is not limited to Nlrp6, as it also occurs in mice deficient in adaptive immunity, which have been repeatedly shown to feature microbiome aberrations under conventional housing conditions (Garrett et al., 2007; Kawamoto et al., 2014; Zhang et al., 2015). Altogether, this highlights that, under eSPF conditions, a stable genotype-independent bacterial community can be maintained in immunocompromised mice within a facility.

Introduction of Potential Pathobionts into Immunodeficient Mice Reveals Host Genetics-Driven Effects on the Microbiome

We hypothesized that unaltered microbiota composition in immunodeficient mice housed in eSPF conditions may result from the absence of distinct bacteria that are able to explore specific ecological niches opened as a consequence of altered host immune function. Therefore, we introduced the microbiota of conventionally housed dysbiotic *Nlrp6*$^{-/-}$ mice (Conv-Dys) (Elinav et al., 2011) into eSPF WT, *Rag2*$^{-/-}$, and *Nlrp6*$^{-/-}$ mice through fecal transplantation (FT) (Figure 3A). Comparison of fecal microbiota composition before (eSPF) and after (eSPF+Conv-Dys) FT revealed two main clusters, one comprising mice before challenge and another one comprising mice receiving the FT as well as the donor mice (Figure 3B). Analysis of OTUs present in recipients and donor mice demonstrated that 86% of the OTUs from the donor community were being transferred into all three recipient lines (Figure 3C). Within the cluster of FT recipient mice, further sub-clustering was observed (Figure 3D), and pairwise comparisons between WT and gene-deficient mice revealed no significant genotype-driven difference between WT and *Nlrp6*$^{-/-}$ mice using fecal DNA after 4 weeks, but between WT and *Rag2*$^{-/-}$ mice (Figures 3E and 3F). Since Nlrp6 has been proposed to specifically modulate the mucosal barrier (Levy et al., 2015; Wlodarska et al., 2014), we next investigated the microbiota composition in the intestinal lumen or the mucus layer of *Nlrp6*$^{-/-}$ and *Rag2*$^{-/-}$ mice. Moreover, in order to distinguish metabolically active from inactive bacteria with high sensitivity, we performed 16S rRNA gene sequencing based on RNA rather than DNA (Berry et al., 2012; Emerson et al., 2017; Rodríguez-Blanco et al., 2009). RNA was isolated from luminal and mucosa-associated bacteria at four different anatomic sites: i.e., ileum (SI), cecum (Cec), proximal colon (PC), and distal colon (DC). Comparative analysis of DNA- versus RNA-based microbiota analysis is described in Figure S3A. Analysis of 16S rRNA sequencing data using NMDS showed several distinct clusters reflecting the different genotypes and anatomical sites (Figure 3G). Testing with ADONIS indicated that the variable "GI location" contributes 67% to the observed variability ($R^2 = 0.675$, $p < 0.001$), followed by the variable "genotype," which explained 7% ($R^2 = 0.070$, $p < 0.001$) (Figure 3G). Similar effects were observed when separating samples into luminal and mucosa-associated bacteria, with the community in Rag-deficient mice clustering distinctively from WT and *Nlrp6*$^{-/-}$ mice (Figures 3H and 3I). After FT, the microbial relative abundance was dominated by Clostridiales, Bacteroidales, Campylobacterales, and Deferribacterales, which represent 98% of the bacteria found at different GI sites (Figures S3B–S3D). In the lumen, "GI location" and "genotype" have a significant effect ($R^2 = 0.528$ and $R^2 = 0.127$, respectively; $p < 0.001$). In the mucosa, "GI location" presented a higher contribution in comparison with the lumen ($R^2 = 0.699$, $p < 0.001$), and "genotype" also contributed, to a lower degree, to the differences ($R^2 = 0.0615$, $p < 0.001$). Pairwise comparisons of WT and *Nlrp6*$^{-/-}$ mice revealed that communities in the colon, but not cecum and SI, differed significantly, with "genotype" explaining up to 41% of variability, i.e., in the lumen of the DC (Figure S4). Communities in *Rag2*$^{-/-}$ mice differed at most sites, except the lumen of the small intestine and the mucosa in the DC, from the ones in WT mice (Figure S4). This demonstrates that, upon exposure to pathobiont-containing communities, deficiencies in adaptive immune cells have a broad impact on microbiota composition, while deficiency in Nlrp6 has a rather distinctive, but readily detectable, influence on the metabolically active communities in the colon.

Increased Abundance of Pathobionts in Mice Deficient of Nlrp6 and Adaptive Immunity

We next explored the taxonomic composition of the bacteria, which differs between genotypes in the lumen of the colon. For this analysis, we included data from two independent FT experiments, i.e., transfer of Conv-DysM microbiota into eSPF mice (WT, *Rag2*$^{-/-}$, and *Nlrp6*$^{-/-}$), and employed complementary statistical approaches to identify biomarkers at higher taxonomic levels by the linear discriminant analysis (as described in linear discriminant analysis effect size [LEfSe]) (Segata et al., 2011) and differentially abundant (DA) OTUs using the negative binomial Wald test (as described in Love et al., [2014]). Initial NMDS analysis confirmed that samples readily clustered by genotype in the lumen of the proximal and DC, which was corroborated by statistical analysis (ADONIS, $R^2 > 0.10$; $p < 0.01$) (Figures 4A–4D). We next performed LEfSe analysis (linear discriminant analysis [LDA] score > 3.0) to identify DA bacterial families at the different sites in the colon. In the DC of *Nlrp6*$^{-/-}$ mice, the families of Helicobacteraceae, Deferribacteraceae, and Desulfovibrinaceae were enriched, while Lactobacillaceae and Bacteroidaceae were reduced (Figure 4B;

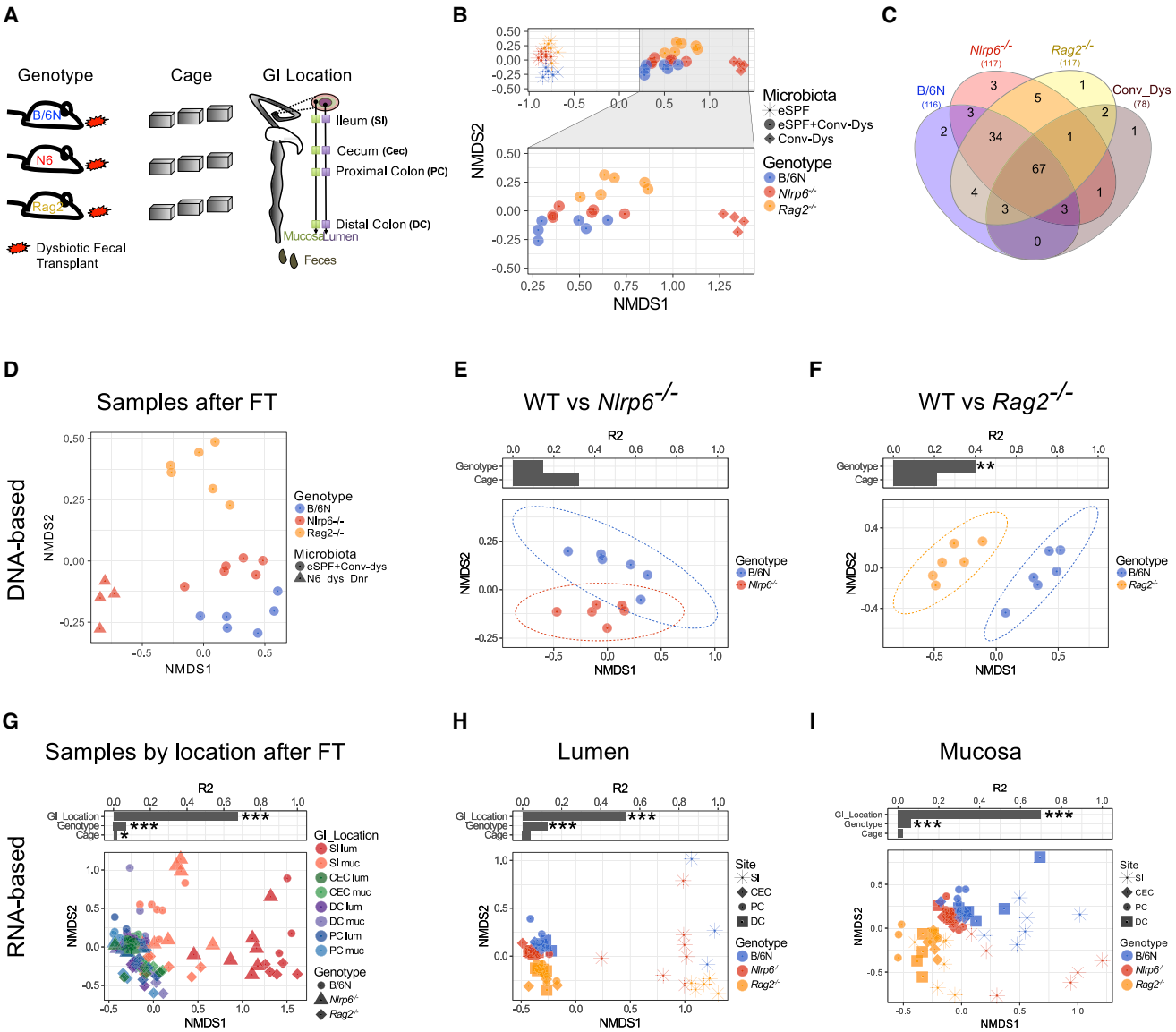

Figure 3. GI Location and Host Genotype Regulate Spatial Organization of the Gut Microbiome

(A) Scheme for dysbiotic microbiota transfer experiment. WT (B/6N), *Nlrp6*$^{-/-}$ (N6), and *Rag2*$^{-/-}$, (Rag2) mice bred in eSPF conditions were subjected to a fecal transplantation (FT) from conventionally housed *Nlrp6*$^{-/-}$ mice. Fecal samples were taken before and 4 weeks after FT for DNA isolation. Luminal and mucosa-associated samples for RNA isolation were taken from indicated locations (GI locations) 4 weeks after FT.

(B) NMDS ordination analysis of microbiota composition using Bray-Curtis distances from fecal DNA of donor *Nlrp6*$^{-/-}$ mice (Conv-Dys) and recipient mice before (eSPF) and after FT (eSPF+Conv-Dys). The zoomed section includes mice after FT as well as donor mice.

(C) Venn diagram indicating the number of shared OTUs between the donor mice and the FT recipients.

(D–F) NMDS of fecal samples after FT using DNA as template (D). NMDS analysis and individual effect size of "genotype" and "cage" using pairwise comparison in *Nlrp6*$^{-/-}$ versus WT mice (E) and *Rag2*$^{-/-}$ versus WT mice (F).

(G–I) NMDS of samples across the GI tract after FT using RNA as template. NMDS ordination and effect size of GI location, genotype, and cage in all samples (G), from lumen (H), or from mucosa (I).

Permutational multivariate ANOVA (ADONIS) was used to calculate the variance explained by individual factors in (E) and (F). *$p < 0.05$; **$p < 0.01$; ***$p < 0.001$.

Table S1). A similar observation was made for the DC of *Rag2*$^{-/-}$ mice (Figure 4D). Notably, a different pattern was detected in the PC of *Nlrp6*$^{-/-}$ mice showing an enrichment of Porphyromonadaceae and a decrease in the little described family/cluster Bacteroidales S24-7 (Figure 4A), while the DA bacteria in the PC of Rag mice resembled the ones in the DC (Figure 4C). We then performed an analysis of DA OTUs using DESeq2 (log_2 fold change > 2.0; $p < 0.05$, after correction for multiple test) for the PC and DC, comparing each gene-deficient mouse line separately against WT mice. For *Nlrp6*$^{-/-}$ mice, we identified 23 (PC, 13 up and 10 down) and 24 (DC, 15 up and 9 down) distinct DA OTUs (Figures 4A and 4B). In *Rag2*$^{-/-}$ mice, we identified 86

(legend on next page)

(PC, 26 up and 60 down) and 70 (DC, 22 up and 48 down) distinct DA OTUs (Figures 4C and 4D). Taking the results presented earlier, we investigated whether certain microbial taxa could be associated with immune deficiencies. To identify whether particular OTUs are associated to *Nlrp6*$^{-/-}$ as well as Rag2$^{-/-}$, we identify the fraction of shared OTUs from a total of 41 distinct OTUs enriched in gene-deficient mice and then the ones shared between the different colonic sites of *Rag2*$^{-/-}$ and *Nlrp6*$^{-/-}$ mice, respectively (Figure 5A; Table S2). In total, 9 OTUs were enriched in at least one site in both *Rag2*$^{-/-}$ and *Nlrp6*$^{-/-}$ mice, but only 2 (OTU_198 and OTU_96) were enriched in all sites. The first OTU belongs to a member of the Helicobacteraceae family (closest match, *Helicobacter typhlonius* strain MIT 97-6810, 99% of identity, NCBI BLAST), and the second belongs to a member of the Clostridiaceae family (closest match, *Butyricicoccus pullicaecorum* strain 25-3, 96% of identity, NCBI BLAST) (Figure 5B; Table S3). Additional OTUs that were partially shared included *Mucispirillum schaedleri* OTU_37 (strain HRI I17, 100% of identity), *Desulfovibrio* OTU_112 (closest match, *Desulfovibrio desulfuricans*, 90% of identity), and OTU_454 (unknown *Lachnospiraceae* UCG-001) (Figure 5C). Notably, Prevotellaceae did not have significant changes in their relative abundances (Figure S5). The relative low number of shared DA OTUs between gene-deficient mice (9 of 41) supports the model that specific OTUs are able to explore distinct niches opened as a consequence of impaired host immunity. However, notably, the shared OTUs are enriched in potential pathobionts from the phylum Proteobacteria, suggesting that these bacteria potentially benefit from deficiencies in Nlrp6 and adaptive immunity.

Besides its function as inflammasome sensor, Nlrp6 has been demonstrated to regulate nuclear factor κB (NF-κB) and mitogen-activated protein kinase (MAPK) signaling as well as to contribute to antiviral effector functions (Anand et al., 2012; Grenier et al., 2002; Levy et al., 2017). Particularly, the Nlrp6-mediated regulation of interleukin (IL)-18 processing, resulting in the induction of antimicrobial peptides, has been shown to contribute to shaping the microbiome (Levy et al., 2015). Hence, we assessed the expression of inflammasome components as well as inflammasome activation in differing housing conditions. Specifically, we measured the concentration of active IL-18 and the gene expression of *Nlrp6*, *Casp1*, and *Il18* in the colon of WT and *Nlrp6*$^{-/-}$ mice housed under conventional and eSPF conditions as well as 4 weeks after reintroduction of the dysbiotic community. In line with earlier findings, active IL-18 was reduced 3- to 4-fold in conventionally housed *Nlrp6*$^{-/-}$ mice, compared to WT mice housed in the same room (Figure S5). The expression levels of *Casp1* and *Il18* only showed minor differences between all housing conditions, suggesting that the amount of active IL-18 in the colonic tissue is regulated by differential post-translation processing via caspase-1 and not via differential gene expression in conventional housing conditions, supporting recent observations (Levy et al., 2015). In contrast, both lines of mice did not differ in colonic IL-18 production in eSPF conditions or after FT (eSPF+Conv-Dys). Notably, in eSPF conditions, colonic IL-18 was relatively lower compared to conventional conditions and increased upon FT, independent of Nlrp6, to comparable levels observed in conventionally housed WT mice. This suggests that inflammasome-independent effects of Nlrp6 may be responsible for the observed effect on the microbiota or that Nlrp6 controls intestinal inflammasome activation only during specific periods after colonization, which should be carefully investigated in future studies involving time-resolved global immune monitoring under differing housing conditions.

Together, our observation that the abundances of DA OTUs vary strongly at different anatomical sites reiterates the notion that specific immune mechanisms, as well as environmental and ecological parameters, shape microbial colonization throughout the GI tract.

DISCUSSION

Laboratory animals are an essential experimental model for investigating the interplay between host and microbiota, and our knowledge of the complexity of host-microbiota interaction in laboratory animals is still growing (Rausch et al., 2016; Roy et al., 2017; Stappenbeck and Virgin, 2016; Thiemann et al., 2017). Importantly, previously underappreciated environmental factors have been identified to strongly influence the microbiome composition; hence, cofounding effects derived from these environmental factors may have led inadvertently to misinterpretations of results in animal experimentation, e.g., we recently demonstrated that microbiota normalization in WT and gene-deficient mice is able to reconcile the opposing functions of caspase-1 during chemically induced colitis (Błażejewski et al., 2017). Specifically, familial transmission, i.e., vertical transmission of the microbiome from mothers to their offspring, and exposure to specific communities have been suggested to be large cofounding factors when investigating the influence of the host genotype on the microbiome (Ubeda et al., 2012). Using a cross-sectional approach, we previously identified an altered microbiota composition in Nlrp6 inflammasome-deficient mice (Elinav et al., 2011). Subsequent studies concluded that impaired goblet cell function and reduced secretion of antimicrobial

Figure 4. Increased Abundance of Distinct Bacteria in Distal Colon of eSPF+Conv-Dys *Nlrp6*$^{-/-}$ and *Rag2*$^{-/-}$ Mice

RNA-based microbiome analysis in the proximal colon (PC) and distal colon (DC) of two cohorts of eSPF WT, *Nlrp6*$^{-/-}$, and *Rag2*$^{-/-}$ mice 4 weeks after receiving independent FT from Conv-Dys *Nlrp6*$^{-/-}$ mice.

(A–D) Active communities were analyzed using NMDS, LEfSe, and DESeq2. After LEfSe analysis, bacterial families with LDA scores > 3.0 are displayed. Log ratio and mean average (MA) plots were used to visualize DA OTUs (up: red; down: blue; $p < 0.05$ after correction for multiple tests) identified using DESeq2. (A and B) Analysis of active communities in PC (A) and DC (B) of WT and *Nlrp6*$^{-/-}$ mice. (C and D) Analysis of active communities in PC (C) and DC (D) of WT and *Nlrp6*$^{-/-}$ mice.

Data shown summarize two independent experiments. Permutational multivariate ANOVA (ADONIS) was used to calculate the variance explained by individual factors in (A) and (D). A significant effect was attributed when $p < 0.05$ and $R^2 > 0.10$ (equivalent to 10% of explained variance).

*$p < 0.05$; **$p < 0.01$; ***$p < 0.001$.

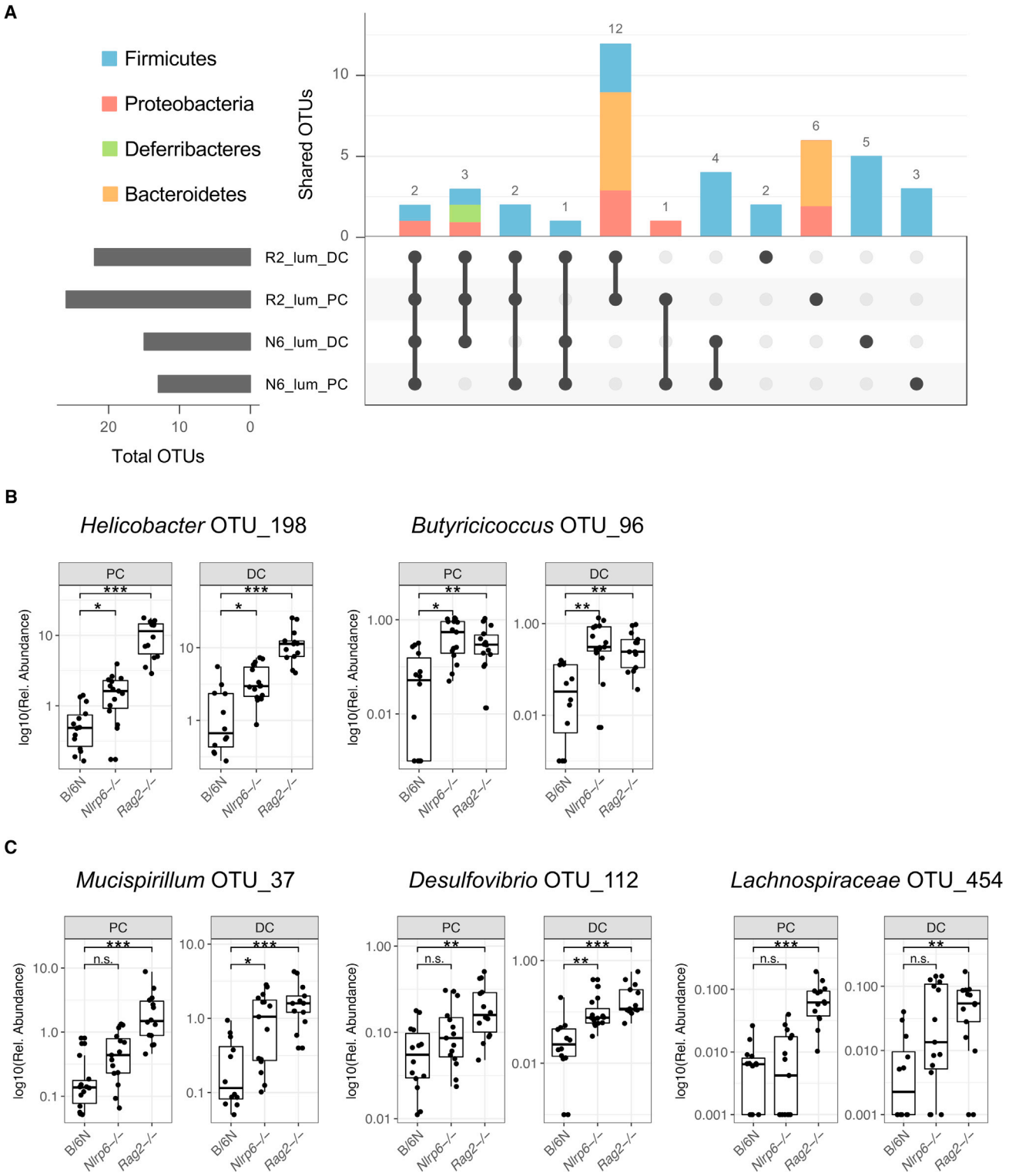

Figure 5. Distinct Commensals Explore Specific Niches in Immunodeficient Mice

RNA-based microbiome analysis in the PC and DC of two cohorts of eSPF WT, *Nlrp6*$^{-/-}$, and *Rag2*$^{-/-}$ mice 4 weeks after receiving independent FT from Conv-Dys *Nlrp6*$^{-/-}$ mice.

(legend continued on next page)

peptides contribute to the development of dysbiosis under conventional housing conditions by modulating the mucosal barrier (Levy et al., 2015; Wlodarska et al., 2014). In addition, a recent study by independent investigators demonstrated the specific expansion of the mucus-dwelling bacterium *Akkermansia muciniphilia* in Nlrp6-deficient *Il10*$^{-/-}$ mice and linked it to the enhancement of colitis (Seregin et al., 2017). However, the questions of whether specific microbial communities and environmental conditions are required to trigger imbalanced intestinal communities in Nlrp6-deficient mice had not been addressed. This is of particular interest, since a generalizable impact of the Nlrp6 inflammasome was not observed in a recent study characterizing the microbiome of littermate mice under SPF conditions (Mamantopoulos et al., 2017). By expanding the previously used cross-sectional approach, we identified a significant influence of familial transmission in different colonies of inflammasome-deficient mice. Together, environmental factors such as association with a specific breeding colony and cage explained up to 52% of the variance found in the microbial compositions, while, in contrast, genotype contributed only 27% of the variance. These findings reiterate the notion that familial transmission surpasses the influence of host genotype on microbiome composition in experimental animals and should be considered when designing experiments.

To overcome familial transmission as a cofounding factor, we standardized the microbiota between WT and gene-deficient mice by performing rederivation through ET, using a colony of inbred foster mothers maintained under enhanced hygienic conditions, resulting in a stable microbiota composition (Stehr et al., 2009). Indeed, rederivation of WT and *Nlrp6*$^{-/-}$ mice, as well as of *Rag2*$^{-/-}$, via ET resulted in offspring that did not significantly differ in their microbiota composition, which is in line with the work of Mamantopoulos and colleagues (Mamantopoulos et al., 2017). Moreover, similar observations were made for a large number of mouse lines deficient in components of the inflammasome pathway or adaptive immunity, i.e., B cells and T cells. The lack of large shifts in the microbiota between these mouse lines supports the hypothesis that community structure and exposure to specific pathobionts are required to cause imbalances in the microbiota of immunocompromised mice. To specifically test this hypothesis, we introduced the dysbiotic community containing pathobionts from conventionally housed *Nlrp6*$^{-/-}$ mice into isobiotic WT, *Rag2*$^{-/-}$, and *Nlrp6*$^{-/-}$ mice by FT. Four weeks later, we assessed the metabolically active microbial communities in these mice as a sensitive, recently established readout. Notably, a comparison of live bacteria within the lumen of the DC (DC-lum RNA) and total fecal communities (Feces DNA) revealed a separation of samples based on sampled nucleic acid, and we observed that OTUs belonging to Clostridiales/Lachnospiraceae were enriched in the RNA fraction and that those belonging to Bacteroidales/S24-7 are relatively decreased, similar to what has been recently reported (Berry et al., 2012; Peris-Bondia et al., 2011). Comparing WT, *Rag2*$^{-/-}$, and *Nlrp6*$^{-/-}$ mice, we observed changes in the metabolically active communities in the lumen of the colon, the most pronounced change being an increased relative abundance of putative pathobionts from the families Helicobacteraceae and Desulfovibrionaceae. While the changes in the lumen of *Nlrp6*$^{-/-}$ mice might be caused by imbalances at the mucosal layer, i.e., Helicobacteraceae are highly enriched in the mucosa-associated fraction, it alternatively suggests that Nlrp6 contributes in a hitherto unknown pathway to shape luminal bacterial communities. In parallel to the experiments with *Nlrp6*$^{-/-}$ mice, we introduced the dysbiotic microbiota in mice deficient in adaptive immune cells. Particularly, secretory immunoglobulin (Ig)A contributes to shaping intestinal microbial communities by binding to microbes and preventing attachment to the mucus layer (Slack et al., 2012). In accordance to previous studies (Bunker et al., 2015; Kawamoto et al., 2014; Planer et al., 2016), which had largely focused on fecal samples, enriched OTUs in the lumen and mucosa of the large intestine of *Rag2*$^{-/-}$ mice included Clostridiales (Lachnospiraceae), Burkholderiales (Sutterellaceae), and mucosa-associated bacteria such as Deferribacteraceae (*Mucispirillum schaedleri*). Moreover, similar to *Nlrp6*$^{-/-}$ mice, *Rag2*$^{-/-}$ mice presented a dramatic overexpansion of an OTU highly related (99% of similarity) to *H. typhlonius* was detected, suggesting that, in WT mice, IgA or T cells reduce its colonization. In accordance, sequencing of IgA-coated bacteria revealed that members of this family are highly enriched in the IgA-bound fraction (Palm et al., 2014). Notably, members of the family Prevotellaceae, which were IgA coated in *Nlrp6*$^{-/-}$ mice, were not expanded in *Nlrp6*$^{-/-}$ and *Rag2*$^{-/-}$ mice. This is in line with our previous reports demonstrating that they were rapidly transferred to WT mice by cohousing (Elinav et al., 2011). We hypothesize that the relative abundances of Prevotellaceae in these colonies are potentially determined by microbial interactions within the respective microbial ecosystems. Notably, a network analysis of the microbiome composition in a large number of humans suggested a positive interaction of Prevotella with *Ruminococcus* and *Dialister* (Gorvitovskaia et al., 2016). Of note, OTUs belonging to the genus Prevotella, which were detected in our dataset, did not match to known species (data not shown), currently preventing further investigation into the relationship between host genotype and members of the Prevotellaceae family.

Hence, our detailed analysis of DA bacteria along the GI tract showed genotype-specific patterns, supporting the model that the host genotype contributes to the microbiota composition and that only distinct bacterial species are able to benefit from ecological niches that become available as a consequence of specific immunodeficiencies. We believe that our experiments also help to reconcile the opposing conclusions that have been

(A) Visualization of DA OTUs commonly enriched in *Nlrp6*$^{-/-}$ and *Rag2*$^{-/-}$ mice using UpSetR plot. The upper chart shows the number and taxonomy of shared OTUs that were identified in higher abundance in *Nlrp6*$^{-/-}$ and *Rag2*$^{-/-}$ mice. The matrix in the bottom visualizes the set of intersections represented by the connected dots.

(B and C) Relative abundance of selected DA OTUs in the DC shared between all (B) or at least one (C) luminal site in *Nlrp6*$^{-/-}$ and *Rag2*$^{-/-}$ mice. The p values are from the Mann-Whitney U test, with Benjamini-Hochberg correction for multiple testing.

*$p < 0.05$; **$p < 0.01$; ***$p < 0.001$.

reported regarding the role of Nlrp6 and, potentially, other molecules in shaping the microbiome. Importantly, littermate controls or standardized rederivation of mice followed by housing under well-controlled environmental conditions are required to enable equal exposure to microbes and overcome factors such as familial transmission. However, a failure to observe differences in microbiome composition between WT and gene-deficient mice under specific environmental conditions does not automatically mean that differences do not exist in other facilities, since we show that it may be explained by the absence/presence of distinct bacteria able to explore immunological niches such as *Helicobacter* spp., and *Desulfovibrio* spp. or mucus-associated bacteria such as *Mucispirillum schaedleri* and *Akkermansia muciniphila* that was recently described (Seregin et al., 2017). Future studies investigating the interplay of host genotype and microbiome composition need to take these considerations into account, in particular since today, many animal vivaria strive to maintain experimental mice under enhanced hygienic conditions that limit the exogenous exposure to intestinal bacteria, creating conditions that have recently even been proposed to be unphysiological (Beura et al., 2016; Rosshart et al., 2017).

In summary, our results demonstrate that the effect of Nlrp6, but also adaptive immunity on microbiome composition, depends on microbial community structure, i.e., the presence of pathobionts such as Helicobacteraceae. In the absence of pathobionts, effects of the immune system on microbiota composition are largely absent. Hence, in general, distinct community structures and, particularly, exposure to specific pathobionts are likely required to cause imbalances in the microbiota, as their development depends on specific interactions between commensals, pathobionts, and the host immune system.

EXPERIMENTAL PROCEDURES

Mouse Lines, Housing Conditions, and Rederivation

The generation of *Nlrp3*^{tm1Flv} (*Nlrp3*$^{-/-}$), *Nlrp6*^{tm1Flv} (*Nlrp6*$^{-/-}$), *B6.129-Nlrp3*^{tm1Flv}*-Nlrp6*^{tm1Flv} (*Nlrp3*$^{-/-}$*Nlrp6*$^{-/-}$), *Pycard*^{tm1Flv} (*Asc*$^{-/-}$), *Casp1*^{tm2Flv} (*Casp1*$^{-/-}$), *Casp4*$^{tm1a(KOMP)Wtsi}$ (*Casp11*$^{-/-}$), *Casp1*^{tm1Flv} (*Casp1/11*$^{-/-}$), *Il1b*^{tm1Yiw} (*Il1b*$^{-/-}$), *Il1a*^{tm1Yiw} (*Il1a*$^{-/-}$), *Ighm*^{tm1Cgn} (*muMT*$^{-/-}$), *Tcrb*^{tm1Mom}*Tcrd*^{tm1Mom} (*Tcrb*$^{-/-}$*Tcrd*$^{-/-}$), and *Rag2*^{tm1Fwa} (*Rag2*$^{-/-}$) has been previously described.

Colonies of conventionally housed WT, *Nlrp6*$^{-/-}$, *Asc*$^{-/-}$, *Casp1/11*$^{-/-}$, and *Rag2*$^{-/-}$ mice on a C57BL/6N background were bred and maintained within one large animal facility using standard housing conditions, i.e., housed in individually ventilated cages (IVCs) and provided with sterilized food, water, and bedding from the same source. The distinct colonies of each genotype originally derived from a single colony of mice but were subsequently bred and maintained in separated rooms for time periods ranging from several months to years without exchange between the colonies. For the cross-sectional study, samples were taken from 8- to 12-week-old mice from at least 3 separate cages per colony within a time span of 14 days.

Conventionally housed WT, *Nlrp3*$^{-/-}$, *Nlrp6*$^{-/-}$, *Nlrp3*$^{-/-}$*Nlrp6*$^{-/-}$, *Asc*$^{-/-}$*Casp1*$^{-/-}$, *Casp11*$^{-/-}$, *Casp1/11*$^{-/-}$, *Il1b*$^{-/-}$, *Il1a*$^{-/-}$, *muMT*$^{-/-}$, *Tcrb*$^{-/-}$*Tcrd*$^{-/-}$, and *Rag2*$^{-/-}$ mice on a C57BL/6N background were rederived using CD1d foster mothers by ET at the animal facilities of the Helmholtz Centre for Infection Research (HZI) (Stehr et al., 2009). Foster mothers used for rederivation were taken at different time points from a continuing and self-contained breeding colony. Foster mothers and offspring obtained after rederivations were maintained and bred under eSPF conditions, i.e., housed in IVCs and provided with sterilized food, water, and bedding from the same source. Access to animal rooms was restricted to trained animal caretakers, and all manipulations were performed in class II biosafety cabinets.

All mice were provided with sterilized food and water *ad libitum*. Mice were kept under strict 12-hr:12-hr light:dark cycle (lights on at 7:00 a.m. and off at 7:00 p.m.) and housed in groups of up to 6 mice per cage.

FT and Sample Collection

FT was done using luminal content of conventionally housed *Nlrp6*$^{-/-}$ mice (Elinav et al., 2011), which were derived from "colony 1" and subsequently transferred to and bred within the conventional barrier of the HZI animal facility without losing their dysbiotic microbiota (Roy et al., 2017). Briefly, mice were euthanized, and intestinal content from colon, cecum, and small intestine was pooled in anaerobic BBL thioglycollate medium and transferred to an anaerobic chamber (70% N_2, 20% CO_2, 10% H_2). After homogenization, the luminal content was filtered through a 70-μm cell strainer and centrifuged for 10 min at 500 × g, at 4°C. The bacterial pellet was suspended in anaerobic brain heart infusion (BHI) medium, and each WT, *Nlrp6*$^{-/-}$, and *Rag2*$^{-/-}$ recipient mouse (males, 6–7 weeks old) received an aliquot of the same preparation by oral gavage. Recipient mice were housed in three separate cages per genotype after FT. Four weeks after FT, fecal pellets were collected for DNA extraction as well as luminal content and tissue samples from SI, Cec, PC, and DC for RNA isolation and 16*S* rRNA amplicon sequencing.

DNA and RNA Isolation as well as cDNA Synthesis

For DNA-based 16S rRNA sequencing, fecal pellets were collected and stored at −20°C until processing. DNA was isolated using an established protocol (Turnbaugh et al., 2009). Briefly, each sample was treated with 500 μL extraction buffer (200 mM Tris, 20 mM EDTA, 200 mM NaCl [pH 8.0]), 200 μL 20% SDS, 500 μL phenol:chloroform:isoamyl alcohol (24:24:1), and 100 μL zirconia/silica beads (0.1-mm diameter). Samples were homogenized twice with a bead beater (BioSpec) for 2 min. After precipitation of DNA, crude DNA extracts were resuspended in TE buffer with 100 μg/mL RNase I and column purified to remove PCR inhibitors.

For RNA-based 16S rRNA sequencing, the GI tract was sampled at 4 different sites (SI, Cec, PC, and DC). For each site, luminal content and mucosal tissue were collected separately and homogenized in TriReagent (Molecular Research Center) using a FastPrep-24 Instrument (MP Biomedicals). RNA was isolated according to the manufacturer's instructions and treated with 2 U DNAase I (Ambion) for 25 min at 37°C. One microgram of total RNA was used to generate cDNA (RevertAid Reverse Transcriptase) using random hexamer primers.

16S rDNA Amplification and Sequencing

Amplification of the V4 region (F515/R806) of the 16S rRNA gene was performed according to previously described protocols (Caporaso et al., 2011). Briefly, for DNA-based amplicon sequencing, 25 ng DNA was used per PCR reaction (30 μL). For RNA-based amplicon sequencing, 150 pg (luminal samples from cecum/colon), 15 ng (luminal samples from SI) or 150 ng (mucosa-associated samples) of cDNA were used per PCR reaction (30 μL). The PCR conditions consisted of initial denaturation for 30 s at 98°C, followed by 25 cycles (10 s at 98°C, 20 s at 55°C, and 20 s at 72°C). Each sample was amplified in triplicates and subsequently pooled. After normalization, PCR amplicons were sequenced on an Illumina MiSeq platform (PE250).

16S rRNA Analysis

Obtained reads were assembled, quality controlled, and clustered using the Usearch 8.1 software package (http://www.drive5.com/usearch/). Briefly, reads were merged using -fastq_mergepairs with -fastq_maxdiffs 30, and quality filtering was done with fastq_filter (-fastq_maxee 1); minimum read length, 200 bp. The OTU clusters and representative sequences were determined using the UPARSE algorithm (Edgar, 2013), followed by taxonomy assignment using the Silva database v128 (Quast et al., 2013) and the RDP Classifier (Wang et al., 2007), with a bootstrap confidence cutoff of 80%. The OTU absolute abundance table and mapping file were used for statistical analyses and data visualization in the R statistical programming environment (R Core Team (2016) package phyloseq (McMurdie and Holmes, 2013).

Determination of Host Gene and Protein Expression in Colon Tissue

Colons were excised, washed in PBS, and divided into proximal and DC. Two centimeters of DC was cut longitudinally into two samples: one for RNA and other for protein extraction. RNA isolation and cDNA synthesis was performed as described earlier. Real-time PCR was done using the Kapa Probe Fast qPCR kit (Kapa Biosystems) and gene-specific probe sets (*Il18* Mm_00434225_m1; *Casp1* Mm_00438023_m1; and *Nlrp6* Mm_00460229_m1 [Applied Biosystems]; *Hprt* [F: CTGGTGAAAAGGACCTCTCG; R: TGAAGTACTCATTATAGTCAAGGGCA; probe: TGTTGGATACAGGCCAGACTTTGTTGGAT]) on a LightCycler 480 instrument (Roche). PCR conditions were 95°C for 60 s, followed by 40 cycles of 95°C for 3 s and 60°C for 30 s. Data were analyzed using the deltaCt method, with *Hprt* serving as the reference housekeeping gene.

Protein extraction was performed by mechanical homogenization of DC tissue samples in NP-40 buffer, containing protease inhibitors (cOmplete Mini EDTA-free, Roche), using Mini-Beadbeater-96 (BioSpec). Tissue homogenates were further centrifuged (10,000 rpm for 5 min at 4°C), and the supernatants were collected for IL-18 cytokine measurements using the IL-18 ELISA kit (MBL International) according to the manufacturer's instructions.

Statistical Analysis

Statistical analyses were performed using R v3.3.0 (2016-05-03), (http://www.rproject.org) and the packages phyloseq (McMurdie and Holmes, 2013) and ggplot2 (Wickham, 2009). We implemented DESeq2 with the Benjamini-Hochberg multiple testing correction (Love et al., 2014; McMurdie and Holmes, 2014) to identify OTUs that were DA in the gut lumen and mucosa of WT and gene-deficient mice by performing pairwise comparisons. OTUs were considered significantly DA between genotypes if their adjusted p value was < 0.05 and if the estimated 2-fold change was >2 (Love et al., 2014). For Mann-Whitney U tests, p values lower than 0.05 were considered as significant after multiple testing correction (Benjamini-Hochberg false discovery rate correction). The permutational multivariate ANOVA (ADONIS) and analysis of similarities (ANOSIM) were computed with 999 permutations. For ADONIS tests, an $R^2 > 0.1$ (effect size, 10%) and p value < 0.05 were considered as significant. For ANOSIM tests, an $R > 0.2$ and p value < 0.05 were considered as significant. The ANOSIM test was performed for datasets with large differences in group sizes

DATA AND SOFTWARE AVAILABILITY

The accession number for the 16S rDNA sequencing data reported in this paper is NCBI: PRJNA420927 (https://www.ncbi.nlm.nih.gov/bioproject/420927).

SUPPLEMENTAL INFORMATION

Supplemental Information includes five figures and three tables and can be found with this article online at https://doi.org/10.1016/j.celrep.2017.12.027.

ACKNOWLEDGMENTS

The work was supported by the Helmholtz Association (VH-NG-933 to T.S.) and the German Research Foundation (DFG) Priority Program SPP1656 "Intestinal Microbiota - A Microbial Ecosystem at the Edge between Immune Homeostasis and Inflammation" (STR1343/1-1 and STR1343/1-2 to T.S.). The funders had no role in the design of the study, collection, analysis, interpretation of data, or in writing the manuscript.

We thank members of the Strowig laboratory for valuable discussions. We appreciate the excellent technical support of the staff of the animal unit and the genome analytics core facility on the Helmholtz Institute for Infection Research.

AUTHOR CONTRIBUTIONS

E.J.C.G., A.I., and T.S. designed the experiments. A.I. performed the animal experiments. E.J.C.G., A.I., and A.G. performed the sample collection and microbial sequencing preparation. E.J.C.G. performed microbiome and statistical analyses. E.J.C.G., R.F., and T.S. prepared the manuscript, with suggestions from all co-authors.

DECLARATION OF INTERESTS

The authors declare no competing interests.

Received: February 15, 2017
Revised: November 14, 2017
Accepted: December 6, 2017
Published: December 26, 2017

REFERENCES

Anand, P.K., Malireddi, R.K.S., Lukens, J.R., Vogel, P., Bertin, J., Lamkanfi, M., and Kanneganti, T.-D. (2012). NLRP6 negatively regulates innate immunity and host defence against bacterial pathogens. Nature *488*, 389–393.

Berry, D., Schwab, C., Milinovich, G., Reichert, J., Ben Mahfoudh, K., Decker, T., Engel, M., Hai, B., Hainzl, E., Heider, S., et al. (2012). Phylotype-level 16S rRNA analysis reveals new bacterial indicators of health state in acute murine colitis. ISME J. *6*, 2091–2106.

Beura, L.K., Hamilton, S.E., Bi, K., Schenkel, J.M., Odumade, O.A., Casey, K.A., Thompson, E.A., Fraser, K.A., Rosato, P.C., Filali-Mouhim, A., et al. (2016). Normalizing the environment recapitulates adult human immune traits in laboratory mice. Nature *532*, 512–516.

Błażejewski, A.J., Thiemann, S., Schenk, A., Pils, M.C., Gálvez, E.J.C., Roy, U., Heise, U., de Zoete, M.R., Flavell, R.A., and Strowig, T. (2017). Microbiota normalization reveals that canonical caspase-1 activation exacerbates chemically induced intestinal inflammation. Cell Rep. *19*, 2319–2330.

Bunker, J.J., Flynn, T.M., Koval, J.C., Shaw, D.G., Meisel, M., McDonald, B.D., Ishizuka, I.E., Dent, A.L., Wilson, P.C., Jabri, B., et al. (2015). Innate and adaptive humoral responses coat distinct commensal bacteria with immunoglobulin A. Immunity *43*, 541–553.

Caporaso, J.G., Lauber, C.L., Walters, W.A., Berg-Lyons, D., Lozupone, C.A., Turnbaugh, P.J., Fierer, N., and Knight, R. (2011). Global patterns of 16S rRNA diversity at a depth of millions of sequences per sample. Proc. Natl. Acad. Sci. USA (*Suppl 1*), 4516–4522.

Clemente, J.C., Pehrsson, E.C., Blaser, M.J., Sandhu, K., Gao, Z., Wang, B., Magris, M., Hidalgo, G., Contreras, M., Noya-Alarcón, Ó., et al. (2015). The microbiome of uncontacted Amerindians. Sci. Adv. *1*, e1500183.

Elinav, E., Strowig, T., Kau, A.L., Henao-Mejia, J., Thaiss, C.A., Booth, C.J., Peaper, D.R., Bertin, J., Eisenbarth, S.C., Gordon, J.I., and Flavell, R.A. (2011). NLRP6 inflammasome regulates colonic microbial ecology and risk for colitis. Cell *145*, 745–757.

Edgar, R.C. (2013). UPARSE: highly accurate OTU sequences from microbial amplicon reads. Nat. Methods *10*, 996–998.

Emerson, J.B., Adams, R.I., Román, C.M.B., Brooks, B., Coil, D.A., Dahlhausen, K., Ganz, H.H., Hartmann, E.M., Hsu, T., Justice, N.B., et al. (2017). Schrödinger's microbes: tools for distinguishing the living from the dead in microbial ecosystems. Microbiome *5*, 86.

Garrett, W.S., Lord, G.M., Punit, S., Lugo-Villarino, G., Mazmanian, S.K., Ito, S., Glickman, J.N., and Glimcher, L.H. (2007). Communicable ulcerative colitis induced by T-bet deficiency in the innate immune system. Cell *131*, 33–45.

Goodrich, J.K., Waters, J.L., Poole, A.C., Sutter, J.L., Koren, O., Blekhman, R., Beaumont, M., Van Treuren, W., Knight, R., Bell, J.T., et al. (2014). Human genetics shape the gut microbiome. Cell *159*, 789–799.

Gorvitovskaia, A., Holmes, S.P., and Huse, S.M. (2016). Interpreting *Prevotella* and *Bacteroides* as biomarkers of diet and lifestyle. Microbiome *4*, 15.

Grenier, J.M., Wang, L., Manji, G.A., Huang, W.J., Al-Garawi, A., Kelly, R., Carlson, A., Merriam, S., Lora, J.M., Briskin, M., et al. (2002). Functional screening of five PYPAF family members identifies PYPAF5 as a novel regulator of NF-kappaB and caspase-1. FEBS Lett. *530*, 73–78.

Henao-Mejia, J., Elinav, E., Jin, C., Hao, L., Mehal, W.Z., Strowig, T., Thaiss, C.A., Kau, A.L., Eisenbarth, S.C., Jurczak, M.J., et al. (2012). Inflammasome-mediated dysbiosis regulates progression of NAFLD and obesity. Nature *482*, 179–185.

Hu, B., Elinav, E., Huber, S., Strowig, T., Hao, L., Hafemann, A., Jin, C., Wunderlich, C., Wunderlich, T., Eisenbarth, S.C., and Flavell, R.A. (2013). Microbiota-induced activation of epithelial IL-6 signaling links inflammasome-driven inflammation with transmissible cancer. Proc. Natl. Acad. Sci. USA *110*, 9862–9867.

Kawamoto, S., Maruya, M., Kato, L.M., Suda, W., Atarashi, K., Doi, Y., Tsutsui, Y., Qin, H., Honda, K., Okada, T., et al. (2014). Foxp3(+) T cells regulate immunoglobulin a selection and facilitate diversification of bacterial species responsible for immune homeostasis. Immunity *41*, 152–165.

Levy, M., Thaiss, C.A., Zeevi, D., Dohnalová, L., Zilberman-Schapira, G., Mahdi, J.A., David, E., Savidor, A., Korem, T., Herzig, Y., et al. (2015). Microbiota-modulated metabolites shape the intestinal microenvironment by regulating NLRP6 inflammasome signaling. Cell *163*, 1428–1443.

Levy, M., Shapiro, H., Thaiss, C.A., and Elinav, E. (2017). NLRP6: a multifaceted innate immune sensor. Trends Immunol. *38*, 248–260.

Love, M.I., Huber, W., and Anders, S. (2014). Moderated estimation of fold change and dispersion for RNA-seq data with DESeq2. Genome Biol. *15*, 550.

Macpherson, A.J., and McCoy, K.D. (2015). Standardised animal models of host microbial mutualism. Mucosal Immunol. *8*, 476–486.

Mamantopoulos, M., Ronchi, F., Van Hauwermeiren, F., Vieira-Silva, S., Yilmaz, B., Martens, L., Saeys, Y., Drexler, S.K., Yazdi, A.S., Raes, J., et al. (2017). Nlrp6- and ASC-dependent inflammasomes do not shape the commensal gut microbiota composition. Immunity *47*, 339–348.e4.

McMurdie, P.J., and Holmes, S. (2013). phyloseq: an R package for reproducible interactive analysis and graphics of microbiome census data. PLoS ONE *8*, e61217.

McMurdie, P.J., and Holmes, S. (2014). Waste not, want not: why rarefying microbiome data is inadmissible. PLoS Comput. Biol. *10*, e1003531.

Palm, N.W., de Zoete, M.R., Cullen, T.W., Barry, N.A., Stefanowski, J., Hao, L., Degnan, P.H., Hu, J., Peter, I., Zhang, W., et al. (2014). Immunoglobulin A coating identifies colitogenic bacteria in inflammatory bowel disease. Cell *158*, 1000–1010.

Peris-Bondia, F., Latorre, A., Artacho, A., Moya, A., and D'Auria, G. (2011). The active human gut microbiota differs from the total microbiota. PLoS ONE *6*, e22448.

Planer, J.D., Peng, Y., Kau, A.L., Blanton, L.V., Ndao, I.M., Tarr, P.I., Warner, B.B., and Gordon, J.I. (2016). Development of the gut microbiota and mucosal IgA responses in twins and gnotobiotic mice. Nature *534*, 263–266.

Quast, C., Pruesse, E., Yilmaz, P., Gerken, J., Schweer, T., Yarza, P., Peplies, J., and Glöckner, F.O. (2013). The SILVA ribosomal RNA gene database project: improvded data processing and web-based tools. Nucleic Acids Res *41*, D590–D596.

R Core Team (2016). R: A language and environment for statistical computing. R Foundation for Statistical Computing: Vienna, Austria. https://www.R-project.org/.

Rausch, P., Basic, M., Batra, A., Bischoff, S.C., Blaut, M., Clavel, T., Gläsner, J., Gopalakrishnan, S., Grassl, G.A., Günther, C., et al. (2016). Analysis of factors contributing to variation in the C57BL/6J fecal microbiota across German animal facilities. Int. J. Med. Microbiol. *306*, 343–355.

Rehman, A., Sina, C., Gavrilova, O., Häsler, R., Ott, S., Baines, J.F., Schreiber, S., and Rosenstiel, P. (2011). Nod2 is essential for temporal development of intestinal microbial communities. Gut *60*, 1354–1362.

Robertson, S.J., Zhou, J.Y., Geddes, K., Rubino, S.J., Cho, J.H., Girardin, S.E., and Philpott, D.J. (2013). Nod1 and Nod2 signaling does not alter the composition of intestinal bacterial communities at homeostasis. Gut Microbes *4*, 222–231.

Rodríguez-Blanco, A., Ghiglione, J.-F., Catala, P., Casamayor, E.O., and Lebaron, P. (2009). Spatial comparison of total vs. active bacterial populations by coupling genetic fingerprinting and clone library analyses in the NW Mediterranean Sea. FEMS Microbiol. Ecol. *67*, 30–42.

Rosshart, S.P., Vassallo, B.G., Angeletti, D., Hutchinson, D.S., Morgan, A.P., Takeda, K., Hickman, H.D., McCulloch, J.A., Badger, J.H., Ajami, N.J., et al. (2017). Wild mouse gut microbiota promotes host fitness and improves disease resistance. Cell *171*, 1015–1028.e13.

Roy, U., Gálvez, E.J.C., Iljazovic, A., Lesker, T.R., Błażejewski, A.J., Pils, M.C., Heise, U., Huber, S., Flavell, R.A., and Strowig, T. (2017). Distinct microbial communities trigger colitis development upon intestinal barrier damage via innate or adaptive immune cells. Cell Rep. *21*, 994–1008.

Segata, N., Izard, J., Waldron, L., Gevers, D., Miropolsky, L., Garrett, W.S., and Huttenhower, C. (2011). Metagenomic biomarker discovery and explanation. Genome Biol. *12*, R60.

Seregin, S.S., Golovchenko, N., Schaf, B., Chen, J., Pudlo, N.A., Mitchell, J., Baxter, N.T., Zhao, L., Schloss, P.D., Martens, E.C., et al. (2017). NLRP6 protects $Il10^{-/-}$ mice from colitis by limiting colonization of *Akkermansia muciniphila*. Cell Rep. *19*, 733–745.

Simon, G.L., and Gorbach, S.L. (1984). Intestinal flora in health and disease. Gastroenterology *86*, 174–193.

Slack, E., Balmer, M.L., Fritz, J.H., and Hapfelmeier, S. (2012). Functional flexibility of intestinal IgA - broadening the fine line. Front. Immunol. *3*, 100.

Sonnenberg, G.F., Monticelli, L.A., Alenghat, T., Fung, T.C., Hutnick, N.A., Kunisawa, J., Shibata, N., Grunberg, S., Sinha, R., Zahm, A.M., et al. (2012). Innate lymphoid cells promote anatomical containment of lymphoid-resident commensal bacteria. Science *336*, 1321–1325.

Stappenbeck, T.S., and Virgin, H.W. (2016). Accounting for reciprocal host-microbiome interactions in experimental science. Nature *534*, 191–199.

Stehr, M., Greweling, M.C., Tischer, S., Singh, M., Blöcker, H., Monner, D.A., and Müller, W. (2009). Charles River altered Schaedler flora (CRASF) remained stable for four years in a mouse colony housed in individually ventilated cages. Lab. Anim. *43*, 362–370.

Thiemann, S., Smit, N., Roy, U., Lesker, T.R., Gálvez, E.J.C., Helmecke, J., Basic, M., Bleich, A., Goodman, A.L., Kalinke, U., et al. (2017). Enhancement of IFNγ production by distinct commensals ameliorates *Salmonella*-induced disease. Cell Host Microbe *21*, 682–694.e5.

Turnbaugh, P.J., Hamady, M., Yatsunenko, T., Cantarel, B.L., Duncan, A., Ley, R.E., Sogin, M.L., Jones, W.J., Roe, B.A., Affourtit, J.P., et al. (2009). A core gut microbiome in obese and lean twins. Nature *457*, 480–484.

Ubeda, C., Lipuma, L., Gobourne, A., Viale, A., Leiner, I., Equinda, M., Khanin, R., and Pamer, E.G. (2012). Familial transmission rather than defective innate immunity shapes the distinct intestinal microbiota of TLR-deficient mice. J. Exp. Med. *209*, 1445–1456.

Vijay-Kumar, M., Aitken, J.D., Carvalho, F.A., Cullender, T.C., Mwangi, S., Srinivasan, S., Sitaraman, S.V., Knight, R., Ley, R.E., and Gewirtz, A.T. (2010). Metabolic syndrome and altered gut microbiota in mice lacking Toll-like receptor 5. Science *328*, 228–231.

Wang, Q., Garrity, G.M., Tiedje, J.M., and Cole, J.R. (2007). Native Bayesian classifier for rapid assignment of rRNA sequences into the new bacterial taxonomy. Appl. Environ. Microbiol. *73*, 5261–5267.

Wickham, H. (2009). ggplot2: Elegant Graphics for Data Analysis (Springer).

Wlodarska, M., Thaiss, C.A., Nowarski, R., Henao-Mejia, J., Zhang, J.P., Brown, E.M., Frankel, G., Levy, M., Katz, M.N., Philbrick, W.M., et al. (2014). NLRP6 inflammasome orchestrates the colonic host-microbial interface by regulating goblet cell mucus secretion. Cell *156*, 1045–1059.

Zhang, H., Sparks, J.B., Karyala, S.V., Settlage, R., and Luo, X.M. (2015). Host adaptive immunity alters gut microbiota. ISME J. *9*, 770–781.